X-ray imaging spectroscopy

Impurity concentration in core plasma with Ross filters method

I. Nick Bogatu

FAR-TECH, Inc.

Presented at US - KSTAR Workshop

General Atomics, San Diego, CA, April 15-16, 2009

X-ray Ross filter (XRF) principle: signal difference is proportional to incident radiation power within the energy pass band ($P_{\Delta E}$) defined by strategically chosen absorption edges

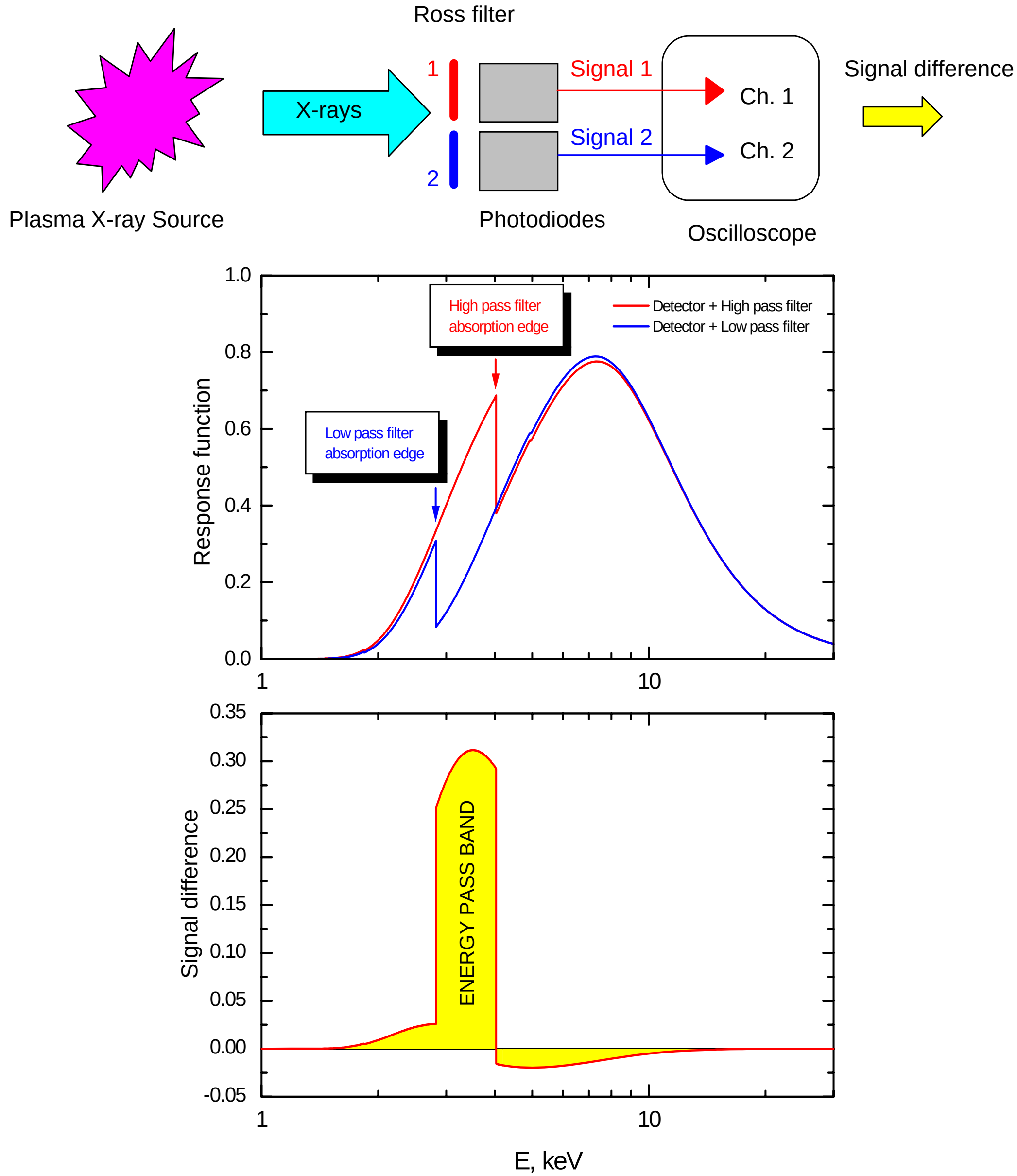

- Can be designed and fabricated for both *lines* and *continuum* X-ray diagnostics, over a *very wide energy range: 0.03 - 115.60 keV*
- *Simple structures* based on photo-absorption effect and *L or K absorption edges*
- *Enough robust* when fixed on rigid frames
- *Work with any kind of X-ray detectors*
- *Very wide acceptance angle* allows large areas of the emission source to be viewed
- The two filtered *signals,* recorded independently, *are processed off-line*
- Pin-hole images provide *time resolved/integrated spectral map* of the lines/ions by processing of the *digital images*
- Considerably *smaller loss of intensity* and the *absence of harmonics* when compared to crystal monochromators
- Can be assembled into *simple and cost-effective spectrometers* for simultaneous *energy, time, and spatial resolution for fast phenomena*

Spectral positions of Ar ions lines(*) determines the selection of the absorption K-edges and the technologically useable materials for XRF design

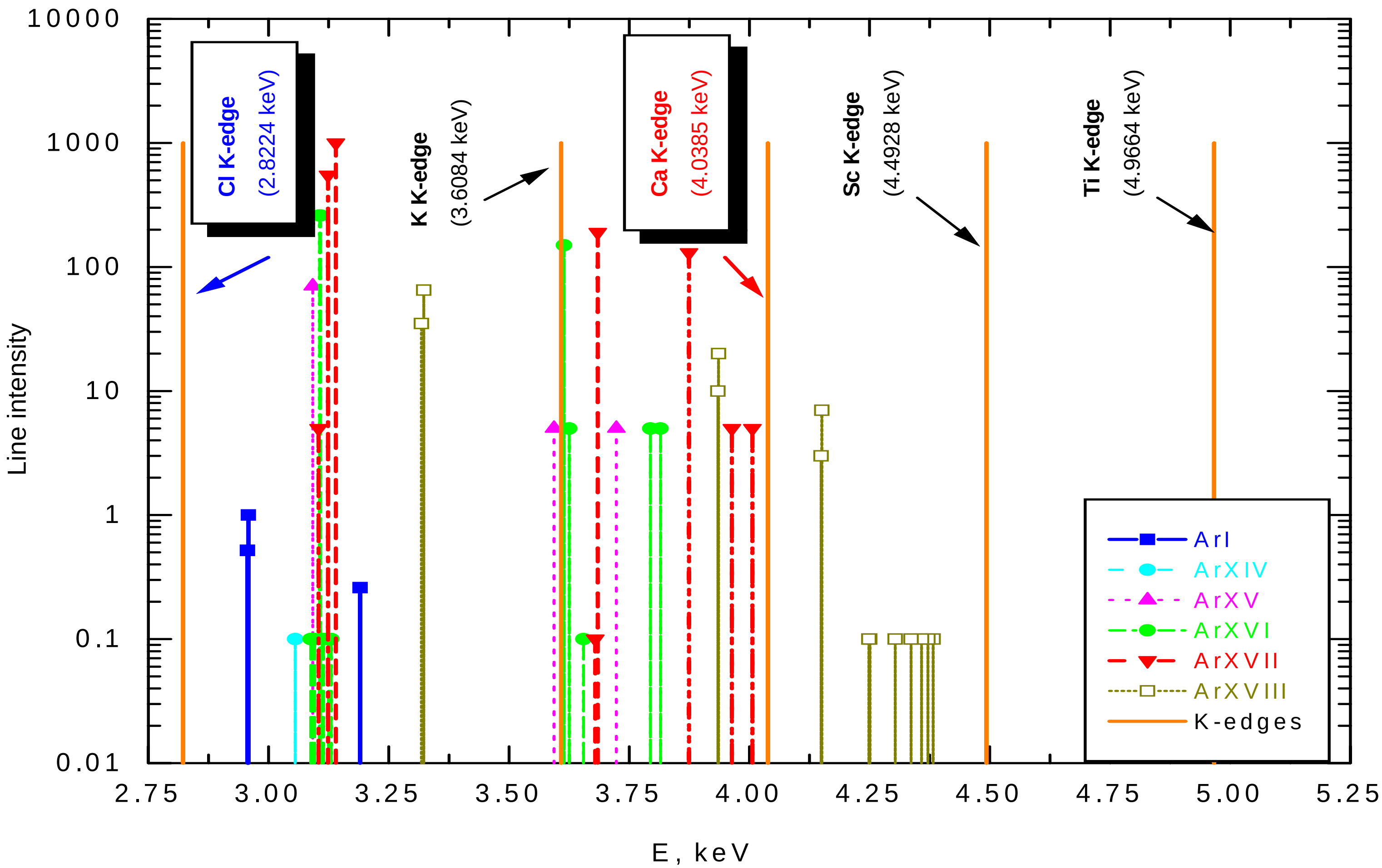

A pass band ΔE = 1.2161 keV is obtained using Ca and Cl K-edges

(*) R.L. Kelly in J. Phys. Chem. Ref. Data **16**, 1987, Suppl No.1

XRF for Ar K_a lines used on DIII-D

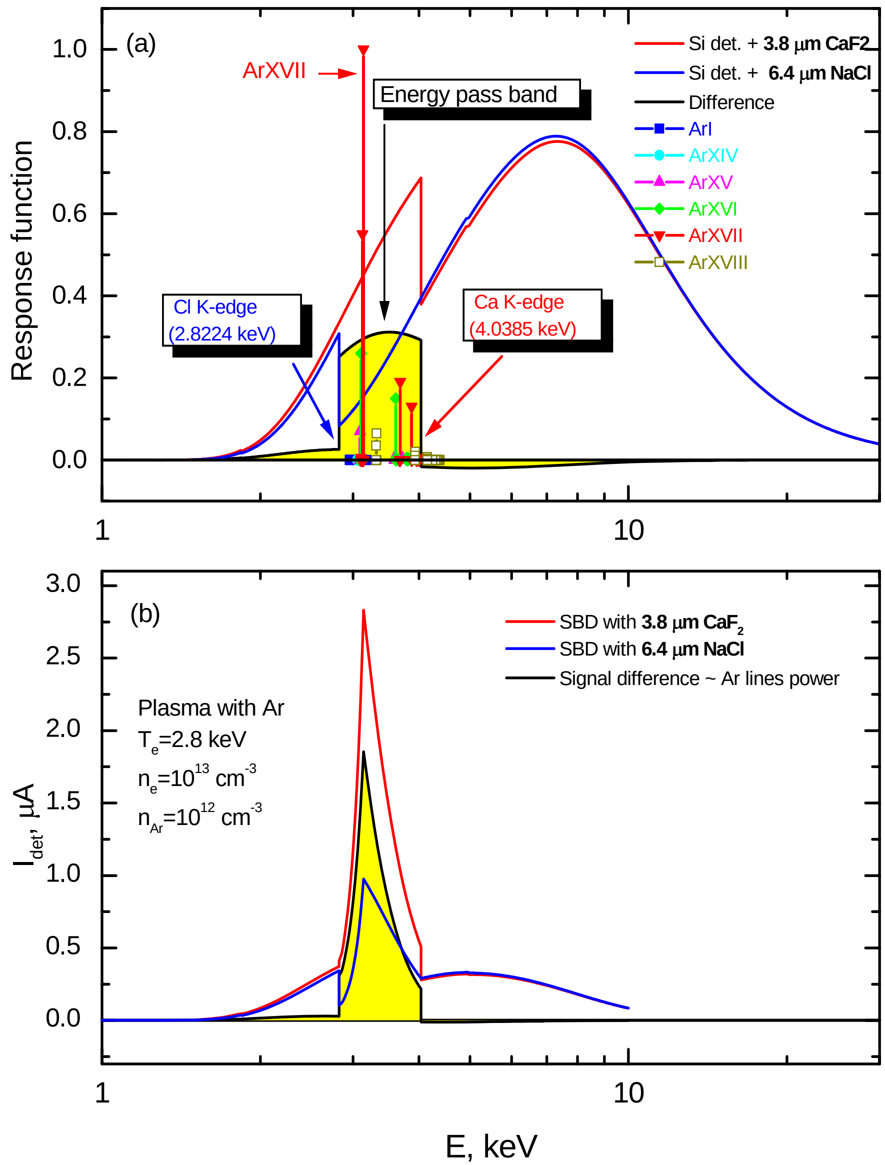

(a) Response function of SBD (150 µm; 0.2 µm Si window) looking at "white spectrum" through 125 µm Be window and the XRF with the structure (10 µm Be support / filter / 0.05 µm Ti protecting layer);

(b) Estimated signal current of this system for plasma with Ar; signal difference is produced only by Ar lines and continuum within the pass band with a relative balance error of 0.05%.

Two SXR toroidal arrays of DIII-D fitted with Ar XRF

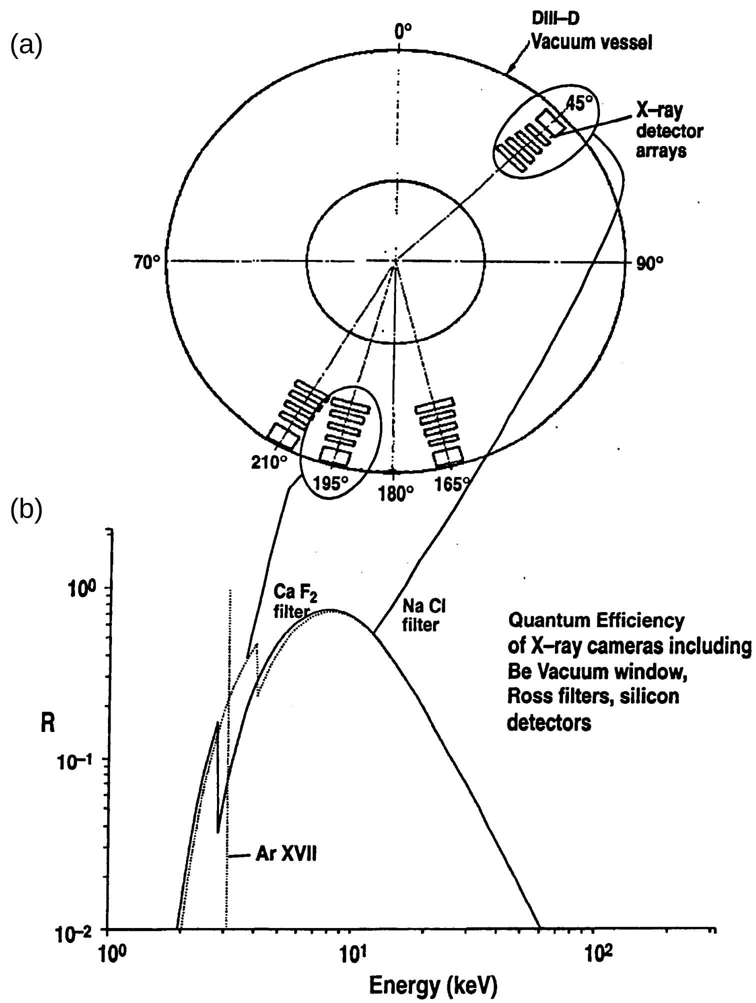

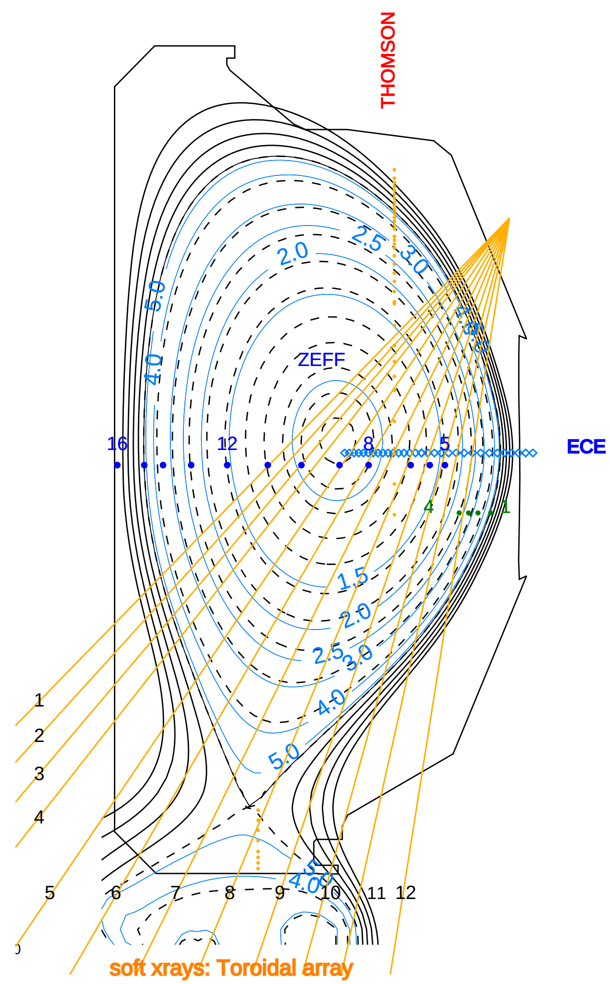

(a) DIII-D X-ray Imaging System

(b) Response function of the silicon detectors equipped with XRF for Ar K_α lines measurements

Discrimination against background and rejection of other impurity radiation, such as Ne, is very good and XRF Ar measurement is very sensitive

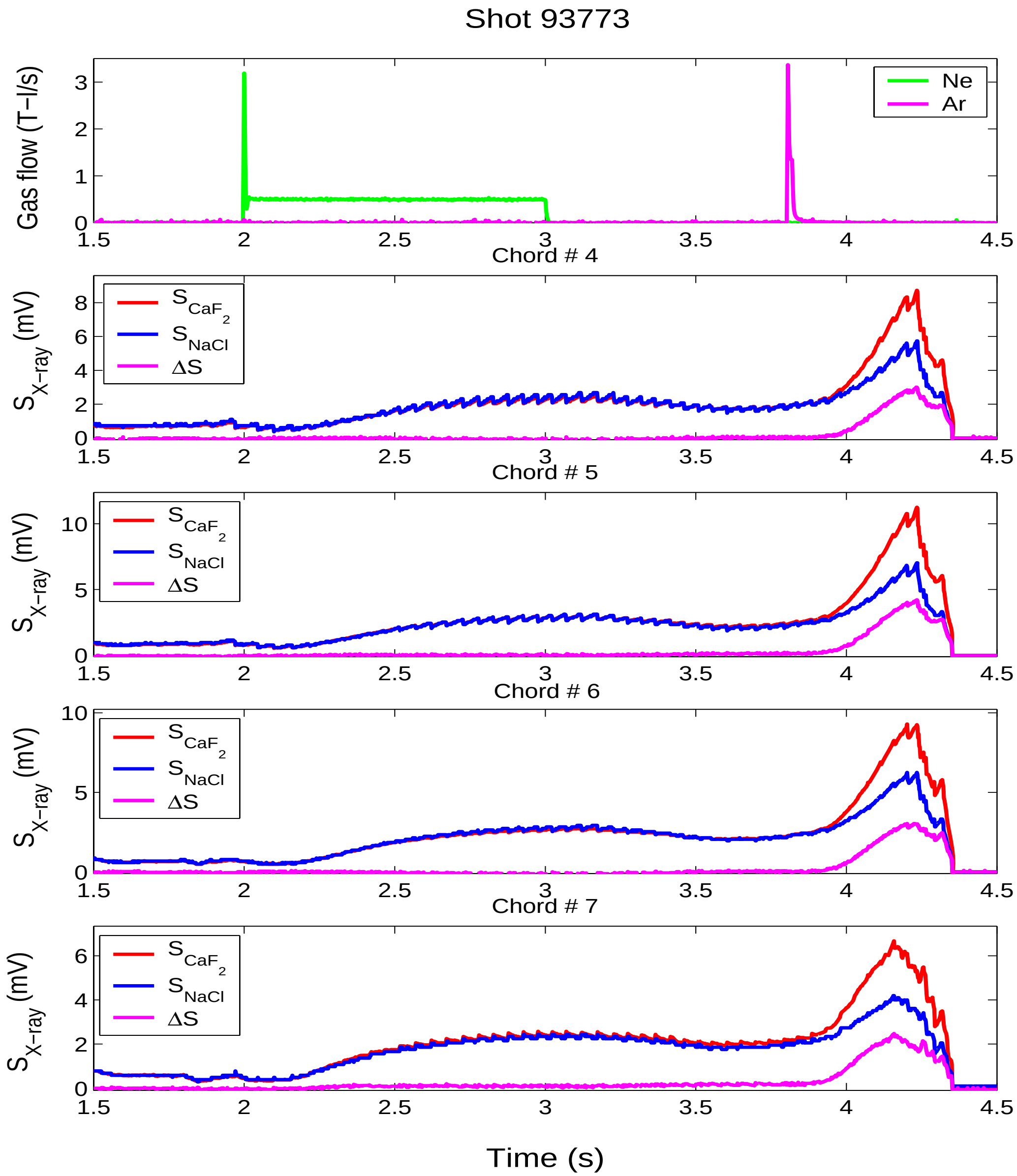

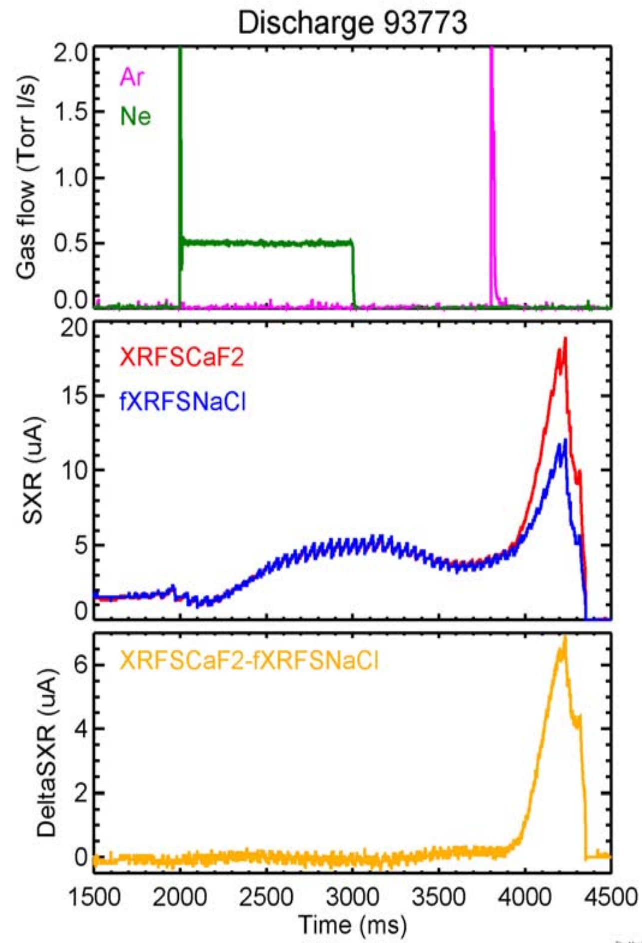

XRF discriminates only Ar brightness, continuum contribution $P_{\Delta E}$ from Ne remains very low and is very sensitive to the injected quantity of Ar

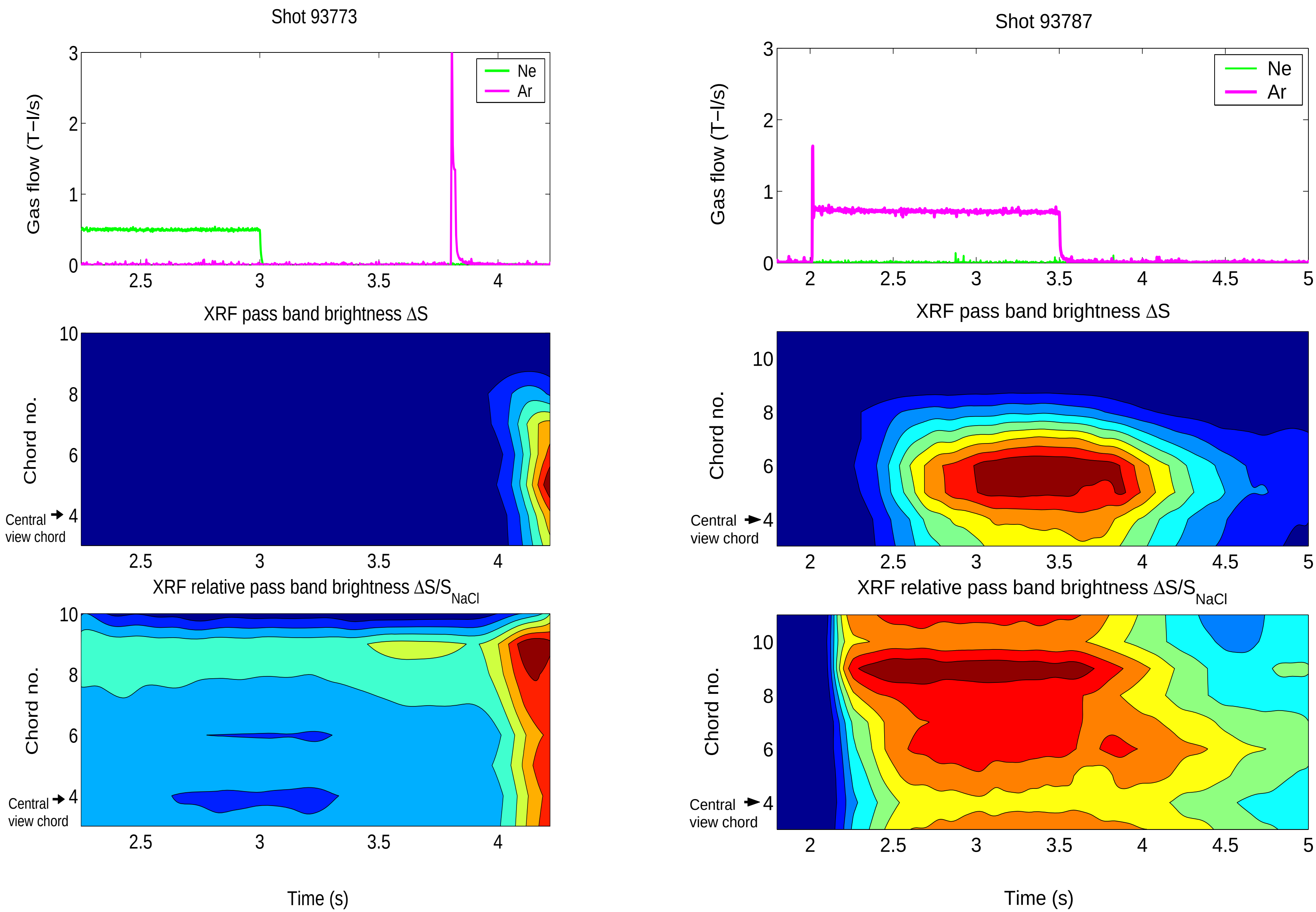

Ar XRF capability demonstrated for puff-and-pump radiating divertor and radiating mantle shots (I_p=1.3 MA, B_T=2.1T, P_{nb}=6.3MW (a) and 6.7MW (b), identical Ar and D gas puffing rates)

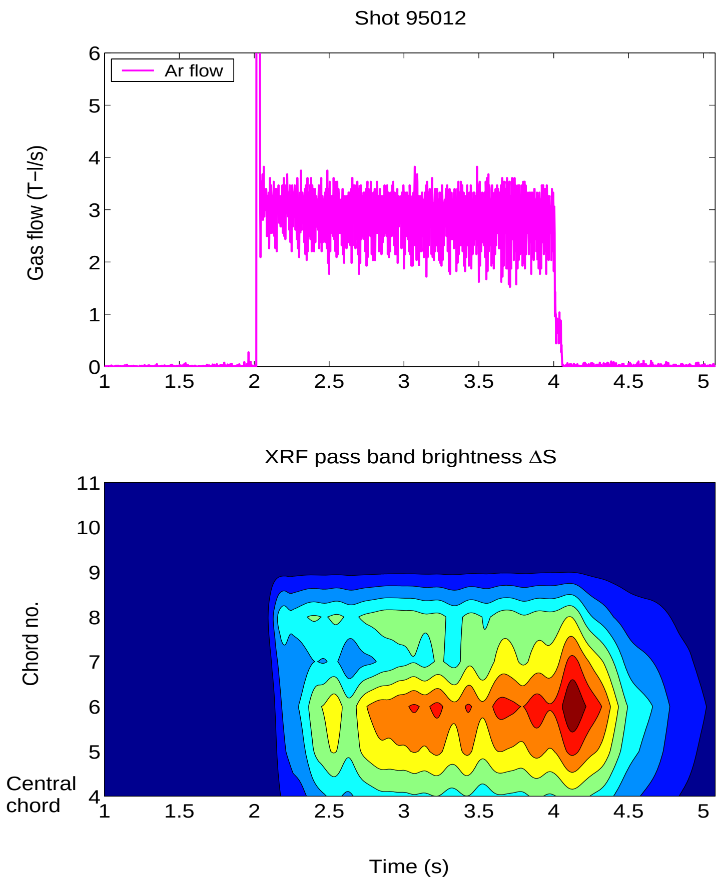

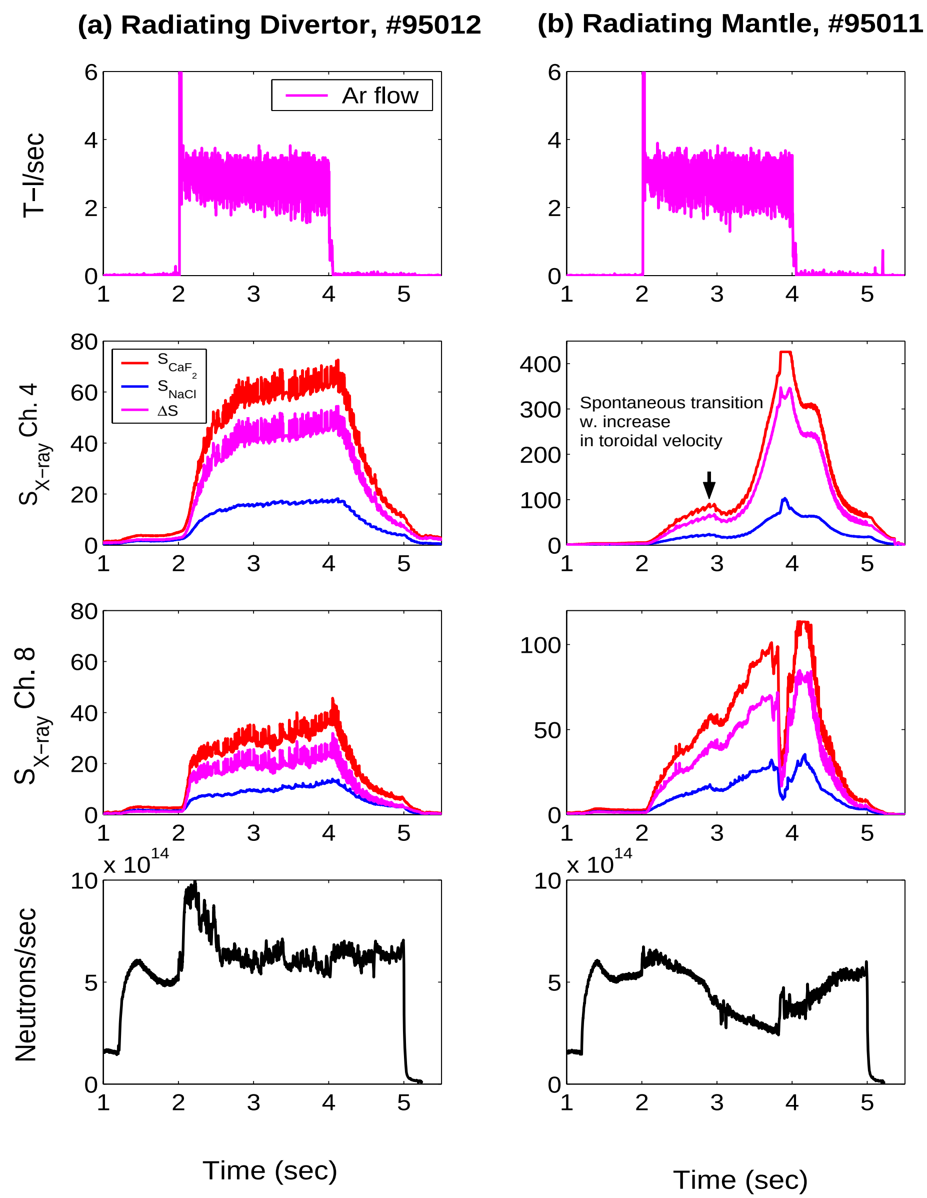

With $T_e(\rho)$ & $n_e(\rho)$ as input for MIST transport code, $D(\rho)$ & $v_c(\rho)$ and core Ar concentration are adjusted so that output matches both CER $Ar^{16+}(\rho)$ and XRF $P_{\Delta E}(\rho)$ simultaneously

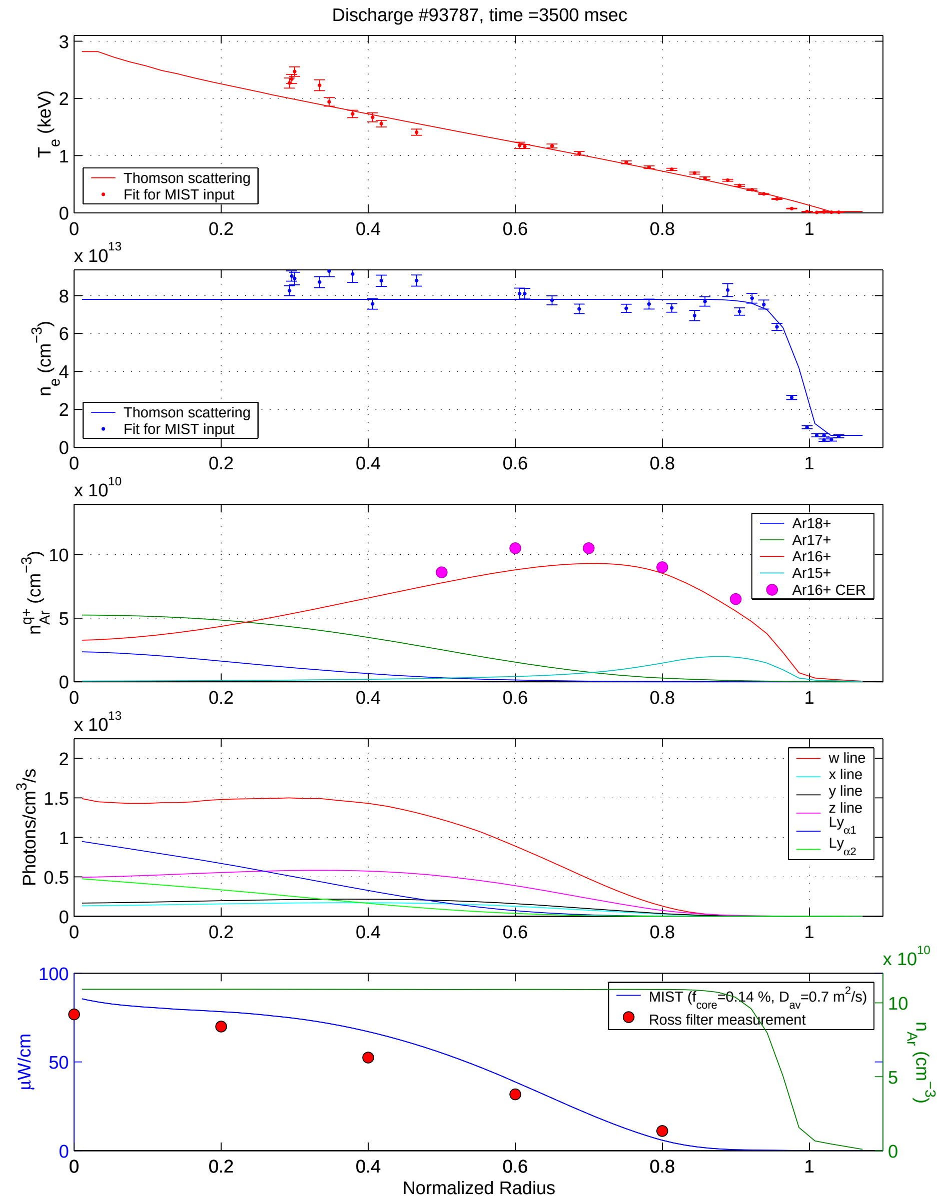

Ar confinement time from transient evolution of Ar concentration after injection ends: ~ 400 ms from XRF and ~ 300 ms from CER Ar^{16+} at ρ ~ 0.7, respectively

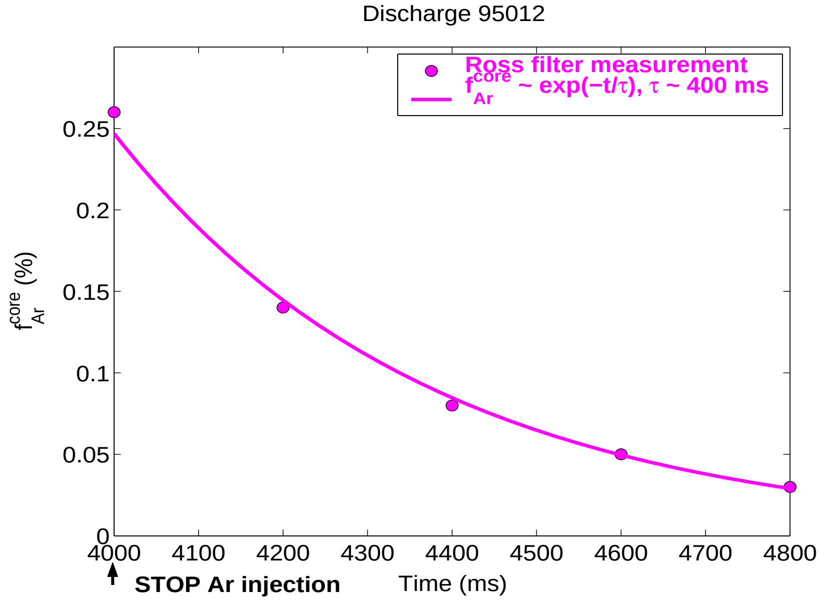

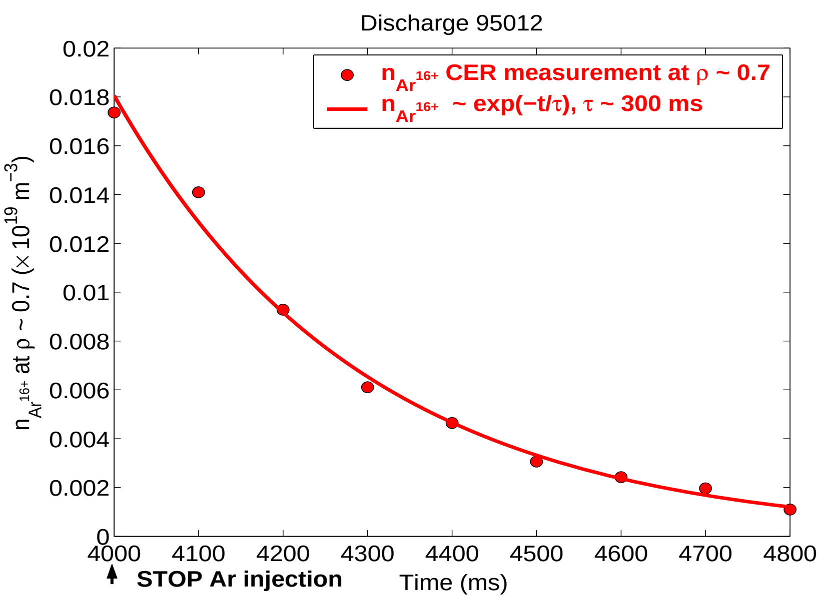

Ar XRF method provides the possibility of investigation of fast phenomena inaccessible to other diagnostics

- **Fast evolution of Ar total concentration in the core plasma in radiating divertor/mantle regime, specifically the effect of sawteeth and ELMs on impurity concentration and the formation of the internal transport barrier**

- **Effect of Ar injected quantity and subsequently the core plasma Ar concentration on the plasma toroidal rotation velocity in different plasma regimes**

- **Investigation of the possibility of validation of multi-chamber model for Ar**
  M.R. Wade et al., Nucl. Fusion **12** (1998) 1839.

- **Comparative experiments, with recycling and non-recycling injected impurities as Ar and K, to study their effects on the divertor, as the same XRF designed for Ar is suitable for K as well**